

# Structure-Function Study Of Porins

Duan P. Chen J. Tang, and Bob Eisenberg

Email: dchen@rush.edu

Department of Molecular Biophysics & Physiology, Rush Medical College, Chicago, Illinois 60612, USA

**Keywords:** Porin, Poisson-Nernst-Planck, electrodiffusion, semiconductor-equation.

## ABSTRACT

Single channel current-voltage (IV) relations were measured from proteins that form channels across the outer membranes of Gram-negative bacteria — porins and their mutants in solutions of KCl. The wild-type porins and some of their specific mutants have known x-rays structures, which lays the foundation for this theoretical work. The ionic strength of KCl ranges from 100mM to 3M. Using the already published electrodiffusion permeation theory [1]–[3], the measured IV relations were analyzed by the Poisson-Nernst-Planck (PNP) formulation. The parameters of the permeation property in the theory are obtained by the least-squares fit to the experimental data and compared to the known structure changes in the wild-type porins and their mutants. The comparison shows that the PNP theory can successfully recover the charge difference between the wild-type and mutants; hence, the theory begins to establish the structure-function relation biological charge transport systems and other macro-molecules.

## 1 Introduction

Ionic channel proteins (cylinder shaped, a few Å in diameter and tens of Å in length), found in lipid membranes of living cells, control the rapid passage of ions and the electrical signaling in living cells. Ionic current is used throughout biological systems to perform key physiological functions, such as, signaling in the nervous system, signal transduction in sensory organs, and coordination of muscle contraction.

Porins are found in the outer membrane proteins of *Escherichia coli* [4]. They form a large water-filled pore in the outer membrane; therefore, they are the pathway for the exchange of most solutes between the external environment and the periplasmic volume of a cell. Some porins are specialized for the transport of oligomeric sugars or nucleosides, and some can function as ion channel as well [5], [6].

The high-resolution atomic structures of porins have been obtained, especially for OmpF porin, which is one of the major outer membrane proteins of *Escherichia*

*coli* [4]. OmpF porin forms a trimeric channel with each monomer forms 16-stranded  $\beta$ -barrel, defining the wall of an independent channel. The overall length of the channel is around 4 nm. The pore of the channel decreases abruptly to the narrowest region (the constriction zone) towards nearly the midway of the channel, from an elliptical cross-section of  $2.7 \times 3.8$  nm approximately to the narrowest constriction zone of  $0.7 \times 1.1$  nm. The constriction zone is formed by the bending of polypeptide loop on each monomer into the center of the pore [7]–[10]. The constriction zone provides necessary molecular sieving effect for the selective transport of certain solutes.

Specifically, the internal loop L3 (from residue 101–131) of the  $\beta$ -barrels constricts the pore to its smallest opening, with residue-119 at the tip of the narrowest region. It is found experimentally that all other colicin N-resistant mutations are at the external loop, except the G119D mutation (porins serve as a cell-surface-exposed receptor for many phages and colicins, see [11] for details). This mutation also yields a greater difference in ionic conductance and charge selectivity, because of two effects: (1) the mutation reduces the narrowest pore region from 4.75Å of OmpF to 3.88Å of G119D; (2) it differs from the wild-type OmpF in net charge by one unit charge due to G to D mutation. Since we estimate the structure difference from the measured channel functions (IV's), hence, using G119D, we will have greater ability to estimate the structure difference from the difference of conduction properties than using other mutants. A small difference in conduction might be overwhelmed by the experimental errors otherwise. To use G119D, it is also because G119D is readily available—both the protein for experiment and the structure for calculation.

## 2 Experiment and Theory

### 2.1 Experiment

Single channel measurements were performed by reconstituted purified porins with Mueller-Rudin type bilayers containing phosphatidylethanolamine, phosphatidylserine and phosphatidylcholine in the ratio 5:3:2 (25 mg of total phospholipid per ml n-decane) [12]. The two sides

of the bilayer are defined as cis and trans, and the trans side is electrically grounded.

Current measurements were made from single porin molecules reconstituted into a painted planar bilayer stretched over a 150  $\mu\text{m}$  aperture, area  $\sim 0.02 \text{ mm}^2$ , separating 4 ml of salt solution in a grounded bilayer chamber and 3 ml of salt solution in a Delrin cup (CD22-150 and BCH-22 from Warner Instrument Corporation, Hamden, CT 06514). Measurements were made using Ag || AgCl electrodes connected to the bathing solution by 3 M KCl-3% agar bridges to minimize liquid junction potentials, a precaution not always taken in measurements of permeation in porin. We use the pClamp software by Axon Instrument (Axon Instrument, Inc., 1101 Chess Drive, Foster City, California 94404) to generate the pulse protocols, collect data, and analyze the data. The data are filtered at 1 KHz, because only the open channel permeation data are of interest here, not gating kinetics.

## 2.2 Theory

PNP describes the transport of charged particles by electrodiffusion, and its formulation reads (after substituting the above definition of chemical potential into the flux formula):

$$-\epsilon_a \Psi''(z) = -\epsilon_a \frac{d}{dz} \left[ \ln \frac{A(z)}{A_0} \right] \frac{d\Psi}{dz} + \frac{2\epsilon_m}{R^2 \ln R/L} [(1 - z/L)\Delta + \Psi(z) - \Psi_{\text{bi}}(L)] + \sum_j z_j e C_j(z) + P(z), \quad (1)$$

$$J_j = -D_j \left[ \frac{dC_j(z)}{dz} + z_j \frac{e}{k_B T} C_j(z) \frac{d\Psi(z)}{dz} \right], \text{ for } j = 1 \dots N, \quad (2)$$

with boundary conditions:  $\Psi(0) = \Psi_{\text{bi}}(0) + V_{\text{appl}}$ ;  $\Psi(L) = \Psi_{\text{bi}}(L)$ ;  $C_j(0) = C_j(l) e^{-z_j e \Psi_{\text{bi}}(0)/k_B T}$ , for  $j = 1 \dots N$ , at  $z = 0$ ;  $C_j(L) = C_j(r) e^{-z_j e \Psi_{\text{bi}}(L)/k_B T}$ , for  $j = 1 \dots N$ , at  $z = L$ , where  $L$  is the length of the channel;  $R$  is the radius;  $P(z)$  is the charge distribution of the channel protein defined in the domain  $[0, L]$ ;  $C_j(l)$  is the concentration in the left bath and;  $C_j(r)$  the concentration in the right bath;  $\epsilon_a$  is the dielectric constant of the aqueous pore;  $\epsilon_m$  is the dielectric constant of the channel protein and the lipid membrane;  $V_{\text{appl}}$  is the applied voltage;  $\Delta = V_{\text{appl}} + \Psi_{\text{bi}}(0) - \Psi_{\text{bi}}(L)$ ; and  $\Psi_{\text{bi}}$  is the usual Donnan potential [13]–[15]. The electric current is then  $I = A \sum_j z_j J_j$ , where  $A(z)$  is the channel cross sectional area, and the  $A_0$  is the unit of area.

The first equation above is the usual Poisson equation reduced to one-dimension, assuming the region is rotational symmetric along the center axis. The first term on the right-hand side is the effect of the variable radius geometry. The second term a geometric dielectric

polarization charge from the finite length of the channel geometry. The third term is the charge carried by the mobile ions, and the fourth term is the charge on the channel protein (see Eq. 1).

The second equation is the ion flux density formula: the flux component from the concentration gradient and that driven by electric field. The combined set of equations are nothing but the drift-diffusion equation used in the semiconductor device modeling, adopted for the channel geometry [3].

In order to use the electrochemistry data in the calculation (incorporating the ion-ion correlation effect in the bulk electrolyte solution), the bath concentrations in the above boundary conditions are replaced with activities. The activity  $a$  is defined as  $a = \gamma C$ , where  $C$  is the ionic concentration and  $\gamma$  is the activity coefficient. The activity coefficient in the baths is taken from Table 19 of [16], and is assumed to be spatially independent throughout the entire region in the calculation.

In the PNP model, the channel proteins and lipid membrane are described as dielectric media ( $\epsilon_m$ ) with a fixed charge distribution ( $P(z)$ ). Each ion species is described by three parameters: valence ( $z_j$ ), diffusion coefficient ( $D_j$ ). Those are the parameters of the theory.

## 3 Results, Discussion and Conclusion

The DC current-voltage relations were measured in fifteen ionic solutions for OmpF and G119D. The fifteen KCl solutions are: For each 100, 250, and 500mM solution in the cis-side (the side a voltage applied), the trans-side ionic strength is change from 100, 250, 500, 1000, to 3000mM separately, yielding a total of 15 different cis and trans ionic concentration pairs. The electrophysiological data have indicated that the monomers in porin channel function independently.

In the calculation, we assume each monomer be azimuthal symmetric to reduce the computational effort (we are aware that diffusion of polar molecules is presumably facilitated by a transverse electric field within the channel [17], [18]). In the one-dimensional approximation, we further divide the pore into five regions (if we follow the radius profile shown in Fig. 1 from left to right): (Region 1) 0 to 6 $\text{\AA}$ , this is a region of uniform pore size, corresponding to a region from one opening of porins to a place in the pore, where the pore size starts to get narrower; (Region 2) 6 $\text{\AA}$  to 21.6 $\text{\AA}$ , the pore size is getting smaller gradually in this region; (Region 3) 21.6 $\text{\AA}$  to 24 $\text{\AA}$ , this corresponds to the constriction region—the narrowest pore region; (Region 4) 24 $\text{\AA}$  to 34.4 $\text{\AA}$ , this is a region in which the pore size is getting larger from the narrowest region to the opening at another end of the porins; (Region 5) 34.4 $\text{\AA}$  to 40 $\text{\AA}$ , this is a region of uniform pore size opening from narrow pore to the aqueous bath on the right hand side.

We assume variables (the dielectric constants, diffusion coefficients, and the fixed charge distribution) be constant in each subregion, that is, we represent variables as a piece-wise constant function in pore of porins. In our experience, a spatially continuous representation of variables yields the same result as that of the representation by the piece-wise functions [19]. Here, we should use piece-wise constant representation of variables for simplicity.

In principle, if variables in each region could take different values, we would have ended up with 25 least-square parameters, since we have two dielectric constants (aqueous pore and the lipid membrane), two diffusion coefficients (for potassium ions and chloride ions), and the fixed charge distribution on porins. However, an intelligent use of knowledge eliminates many free parameters. Since porins are highly aqueous pores (probably why it is called porins), the dielectric constant of the aqueous pore should take the value of that of water. We assume  $\epsilon_a = 80$  and  $\epsilon_m = 4$  in Eq. 1). The diffusion coefficients in Region 1, 2, and 5 should take the values of bulk solutions, in which  $D_K = 1.98 \times 10^{-5}$ ,  $D_{Cl} = 2.03 \times 10^{-5}$  cm<sup>2</sup>/sec [20, p. 79]. Therefore, the continuous monotonic representation of diffusion coefficients from Region 2 to Region 3 and from Region 3 to Region 4 requires us to know only the diffusion coefficient in Region 3. This counts two in the total least-square parameters we have. The x-ray structure data and our electrophysiological data suggests that there is a small surface charge effect discussed in [15]. This fact allows us to set the fixed charges in Region 1 and 5 to zero (even we relax this restriction and set values in Region 1&5 as variable, we will have two more least-squares parameters, making a total of 7). The values in Region 2, 3 and 5 add another three least-square parameters, reducing from possible twenty-five to a total of five least-square parameters. We have made a thorough check for the sensitivity of the parameters in the calculation as in the previous work [21], [19]. The details of the least-squares fit have been described [3].

We have a total of 30 IV's, 15 each for OmpF and G119D. Each set of 15 IV's with a total of 372 measured IV points. To show the current magnitude, the rms current value of the IV points is 95pA for OmpF and 51pA for G119D. ( $I_{rms} = \sqrt{\frac{1}{N} \sum_i \sum_j I_{ij}^2}$ ,  $j$  denotes each IV-point in the same ionic solution,  $i$  denotes different ionic solutions,  $N$  is the total number of IV-points in all solutions). The rms deviation of the least-squares fit ( $\sqrt{\frac{1}{N} \sum_i \sum_j (I_{ij}^{PNP} - I_{ij})^2}$ ) is 12pA, which is equivalent to ~12% error for OmpF. The error is 3.4pA for G119D data, equivalent to 7% overall deviation. The fit to the experimental IV is similar to those in [3], hence, it is not shown here.

Figure 2 shows the diffusion coefficient profiles ob-

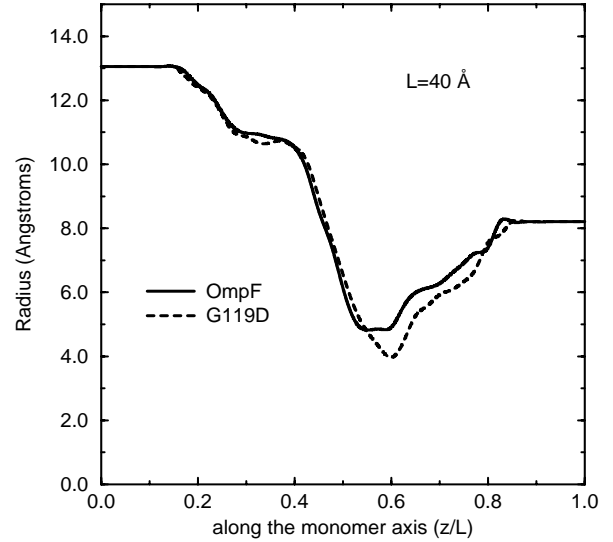


Figure 1: The radius profile along the monomer axis for the wild-type porin OmpF and its mutant G119D. The radius is obtained from the cross sectional area by assuming azimuthal rotational symmetry. The solid-line is for OmpF and the dashed-line is for G119D.

tained by the least-squares fit along the channel pathway for both OmpF and G119D porins. The solid line is for potassium ions in OmpF, and the dashed-line is for chloride ions in OmpF. The solid line with circles is for K<sup>+</sup> in G119D, and the dashed-line with circle is for Cl<sup>-</sup> in G119D. The values of diffusion coefficients reasonably fall down from the bulk value when entering the constriction zone and increase back to the bulk value as leaving the narrow constriction region.

Figure 3 shows the charge distribution profiles obtained by the least-squares calculation. The solid line is for OmpF, and the dashed-line is for G119D. The charge distribution at the two openings is zero for both channels as expected. There is no charge distribution difference in the second region from the left. The only difference in the charge distribution between OmpF and G119d are in the charge constriction region and the fourth region, where there are known structural changes due to the mutation. The net charge on the OmpF is integrated to be 3.132e, and for G119D it is 2.12e. Therefore, a net difference is -1.012e, as expected from G to D mutation.

We conclude that PNP theory can explain the electrostatic effect by the extra negative charge introduced by the mutation from wild-type OmpF porin to G119D, provided that the geometric change from the mutation can be incorporated. We have shown the PNP can be successful in explaining open-channel permeation for porins, and yet to be applied for other biological systems.

## REFERENCES

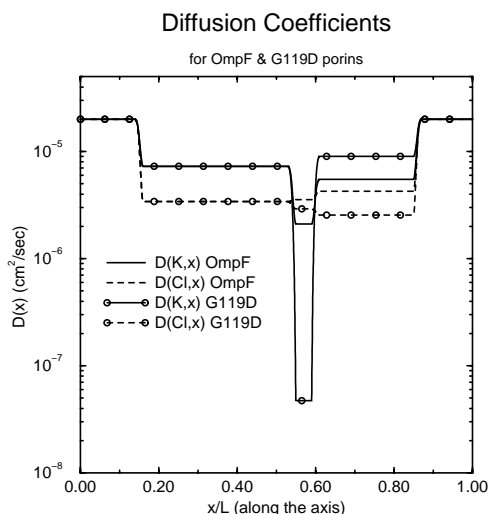


Figure 2: The Diffusion coefficient profiles of potassium ions and chloride ions along the center axis of porin monomer obtained by the least-squares fit for both wild-type OmpF and its mutant G119D. The solid line is for potassium ions in OmpF, and the dashed-line is for chloride ions in OmpF. The solid line with circles is for  $K^+$  in G119D, and the dashed-line with circle is for  $Cl^-$  in G119D.

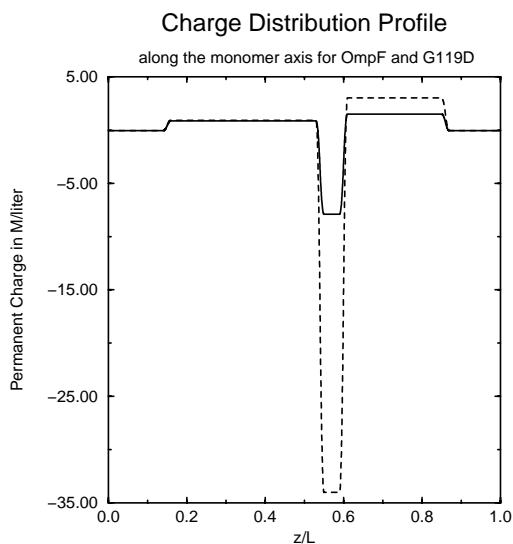


Figure 3: The charge distribution profiles for OmpF and G119D monomer along the center axis are obtained by the least-squares. The solid line is for OmpF, and the dashed-line is for G119D. The integrated areas have yielded a net difference  $-1.012e$ , as expected from G to D mutation.

- [1] V. Barcion, D. P. Chen, R. S. Eisenberg, and J. W. Jerome, *SIAM J. APPL. MATH.* **53**, 631 (1997).
- [2] D. P. Chen, In M. Sokabe, A. Auerbach, and F. Sigworth, editors, *Progress of Cell Research: Towards Molecular Biophysics of Ion Channels*, volume 6 of *Progress in Cell Research*, (Elsevier Science, Amsterdam, 1997). pp. 269–277.
- [3] D. P. Chen, L. Xu, A. Tripathy, G. Meissner, and B. Eisenberg, *Biophys. J.* **76**, 1346 (1999).
- [4] N. H. and M. Vaara, *Microbiol. Rev.* **49**, 1 (1985).
- [5] R. Benz and K. Bauer, *Eur. J. Biochem.* **176**, 1 (1988).
- [6] B. K. Jap and P. J. Walian, *Physiol. Rev.* **76**, 1073 (1996).
- [7] S. W. Cowan, T. Schirmer, G. Rummel, M. Steiert, R. Ghosh, R. A. Paupit, J. N. Jansonius, and J. Rosenbusch, *Nature.* **358**, 727 (1992).
- [8] S. W. Cowan, *Curr. Opin. Struct. Biol.* **3**, 501 (1993).
- [9] K.-L. Lou, N. Saint, A. Prilipov, G. Rummel, S. A. Benson, J. P. Rosenbusch, and T. Schirmer, *J. Biol. Chem.* **271**, 20669 (1996).
- [10] R. Dutzler, G. Rummel, S. Alberti, S. Hernandez-Alles, P. Phale, J. P. Rosenbusch, V. Benedi, and T. Schirmer, *Structure Fold Des.* **7**, 425 (1999).
- [11] D. Jeanteur, T. Schirmer, D. Fourel, V. Simonet, G. Rummel, C. Widmer, J. P. Rosenbusch, F. Pattus, and J.-M. Pagès, *Proc. Natl. Acad. Sci. USA.* **91**, 10675 (1994).
- [12] H. Lee, L. Xu, and G. Meissner, *J. Biol. Chem.* **269**, 13305 (1994).
- [13] D. P. Chen and R. S. Eisenberg, *Biophys. J.* **64**, 1405 (1993).
- [14] S. Selberherr, *Analysis and Simulation of Semiconductor Devices*, (Springer-Verlag, Wien-New York, 1984).
- [15] W. N. Green and O. S. Andersen, *Ann. Rev. Physiol.* **53**, 341 (1991).
- [16] R. A. Robinson and R. H. Stokes, *Electrolyte Solutions*, (Butterworths, London, 2nd edition, 1959).
- [17] M. S. Weiss, U. Abele, J. Weckesser, W. Welte, E. Schiltz, and G. E. Schulz, *Science.* **254**, 1627 (1991).
- [18] A. Karshikoff, V. Spassov, S. W. Cowan, R. Ladenstein, and T. Schirmer, *J. Mol. Biol.* **240**, 372 (1994).
- [19] D. P. Chen, L. Xu, A. Tripathy, G. Meissner, and B. Eisenberg, *Biophys. J.* **73**, 1337 (1997).
- [20] R. Parsons, *Handbook of Electrochemical Constants*, (Butterworths Scientific Publications, London, 1959).
- [21] D. P. Chen, P. Kienker, J. Lear, and B. Eisenberg, *Biophys. J.* **72**, 97 (1997).